

Inhomogeneous Charge Textures Stabilized by Electron-Phonon Interactions in the t-J Model

José Riera¹ and Adriana Moreo²

¹ *Instituto de Física Rosario, Consejo Nacional de*

Investigaciones Científicas y Técnicas, y Departamento de Física,

Universidad Nacional de Rosario, Avenida Pellegrini 250, 2000-Rosario, Argentina and

²*Department of Physics and Astronomy, University of Tennessee, Knoxville, TN 37966-1200 and*
Condensed Matter Sciences Division, Oak Ridge National Laboratory, Oak Ridge, TN 37831-6032

(Dated: October 6, 2018)

We study the effect of diagonal and off-diagonal electron-phonon coupling in the ground state properties of the t-J model. Adiabatic and quantum phonons are considered using Lanczos techniques. Charge tiles and stripe phases with mobile holes (localized holes) are observed at intermediate (large) values of the diagonal electron-phonon coupling. The stripes are stabilized by half-breathing modes, while the tiles arise due to the development of extended breathing modes. Off-diagonal terms destabilize the charge inhomogeneous structures with mobile holes by renormalizing the diagonal coupling but do not produce new phases. Buckling modes are also studied and they seem to induce a gradual phase separation between hole rich and hole poor regions. The pairing correlations are strongly suppressed when the holes are localized. However, in charge inhomogeneous states with mobile holes no dramatic changes, compared with the uniform state, are observed in the pairing correlations indicating that D-wave pairing and moderate electron-phonon interactions can coexist.

PACS numbers: 71.10.Fd, 74.25.Kc, 74.81.-g

I. INTRODUCTION

Electron-phonon interactions (EPI) are at the heart of the pairing mechanism in the BCS theory¹ that successfully describes traditional superconductors. It is believed, however, that EPI cannot produce the high critical temperatures observed in cuprate superconductors and, for this reason, most of the research in the field has focused on the interaction between charge and magnetic degrees of freedom as a source of the pairing mechanism in the cuprates.^{2,3}

Despite almost 20 years of intensive research, the pairing mechanism in the cuprates is still unknown. The experimental evidence indicating that phonons and lattice degrees of freedom play an active role in these materials keeps mounting.^{4,5,6,7} In addition, inhomogeneous structures described as stripes, patches, tiles, etc., have been detected in the underdoped regime of several cuprates.^{7,8,9} The emerging phase complexity is reminiscent of the experimental data for manganites where competing electronic, magnetic and lattice degrees of freedom are responsible for the rich phase structure.¹⁰ It is also likely that the strong electronic correlations present in these materials, in particular the proximity to a Mott insulating phase in the cuprates, could radically change the effects of EPI with respect to those in conventional metals and superconductors.

Most theoretical efforts that tried to incorporate EPI in models for the cuprates were performed in the 90's and they focused on whether the interactions could produce D-wave pairing (instead of S-wave)^{11,12}, and on the tendency of phonons towards the stabilization of charge density wave (CDW) states that could compete with superconductivity (SC). In order to observe CDW states

most of these calculations were performed at quarter filling.^{13,14} Currently, our aim is to understand whether EPI stabilize or destabilize charge stripes, and what kind of inhomogeneous textures, if any, develop. Instead of focusing on the phonons as an alternative source of the pairing mechanism we want to explore whether the interplay of magnetic and phonon interactions with the electrons may lead to an enhancement of the pairing already observed in purely electronic models of high T_c superconductors.¹⁵

In the early studies only diagonal EPI were considered and the effects on hopping terms and Heisenberg coupling due to the lattice distortions (off-diagonal terms) were disregarded. Most of the numerical work was performed with on-site Holstein phonons, and when more extended modes were considered the focus was on breathing modes¹⁴ that would tend to stabilize CDW states and in buckling modes that were known to produce the tilting of the octahedra in YBCO.¹¹ At present, the experimental evidence indicates that the electron-phonon coupling to the breathing mode is strongly anisotropic and, as a result, half-breathing modes seem to have the strongest EPI in the high T_c cuprates.^{5,7} In addition, some authors believe that off-diagonal couplings could be stronger than the diagonal ones.¹⁶

Most of the recent studies of EPI in models for the cuprates have been performed using mean-field, slave-boson, or LDA approximations.^{16,17,18,19} Here, we propose to revisit the t-J model and study the effects of EPI with unbiased numerical techniques. In order to find the relevant phononic modes we will start by studying adiabatic phonons, i.e. $\omega = 0$. Results at finite frequency will be presented for the most relevant modes only.

The paper is organized as follows: Section II describes

the study of adiabatic phonons. Diagonal coupling to breathing modes is discussed in subsection A while subsection B contains results for diagonal coupling to buckling modes. The effect of off-diagonal couplings in both cases is discussed in subsection C. Quantum phonons for the physically important case of half-breathing and buckling modes are discussed in Section III. Conclusions and final remarks are the subject of Section IV.

II. ADIABATIC PHONONS

A. Breathing modes

The Hamiltonian for the t-J model with adiabatic phonons is given by

$$H = - \sum_{\langle \mathbf{i}\mathbf{j} \rangle \sigma} t_{\mathbf{i}\mathbf{j}} (\tilde{c}_{\mathbf{i}\sigma}^\dagger \tilde{c}_{\mathbf{j}\sigma} + \text{h.c.}) + \sum_{\langle \mathbf{i}\mathbf{j} \rangle} J_{\mathbf{i}\mathbf{j}} \mathbf{S}_{\mathbf{i}} \cdot \mathbf{S}_{\mathbf{j}} + H_{e-ph} + H_{ph}, \quad (1a)$$

with

$$H_{e-ph} = \lambda_0 \sum_{\mathbf{i}} u(\mathbf{i}) n_{\mathbf{i}}, \quad (1b)$$

and

$$H_{ph} = \frac{\kappa}{2} \sum_{\mathbf{i}, \mu} (u_{\mathbf{i}, \mu})^2, \quad (1c)$$

where

$$u(\mathbf{i}) = u_{\mathbf{i},x} - u_{\mathbf{i}-\hat{x},x} + u_{\mathbf{i},y} - u_{\mathbf{i}-\hat{y},y}, \quad (2)$$

$$t_{\mathbf{i},\mathbf{j}} = t \{1 + \lambda_t [u(\mathbf{i}) + u(\mathbf{j})]\}, \quad (3)$$

and

$$J_{\mathbf{i},\mathbf{j}} = J \{1 + \lambda_J [u(\mathbf{i}) + u(\mathbf{j})]\}. \quad (4)$$

$\tilde{c}_{\mathbf{i}\sigma}^\dagger$ creates an electron at site $\mathbf{i} = (i_x, i_y)$ of a two dimensional square lattice with spin projection σ ; $\mathbf{S}_{\mathbf{i}}$ is the spin- $\frac{1}{2}$ operator at site \mathbf{i} , $\langle \mathbf{i}\mathbf{j} \rangle$ denotes nearest-neighbor lattice sites, t is the hopping amplitude, and $J > 0$ is the antiferromagnetic exchange coupling. In the following, $t = 1$ and $J = 0.4$ will be adopted unless otherwise stated. Doubly occupancy is not allowed in this model. $n_{\mathbf{i}} = \sum_{\sigma} c_{\mathbf{i}\sigma}^\dagger c_{\mathbf{i}\sigma}$ is the electronic density on site \mathbf{i} . λ_0 is the diagonal electron-phonon coupling and κ is the stiffness constant. λ_t and λ_J are off-diagonal coupling constants for the hopping and Heisenberg interactions respectively. The lattice distortions $u_{\mathbf{i},\mu}$ measure the displacement along the directions $\mu = \hat{x}$ or \hat{y} of oxygen ions located at the center of the lattice's links in the equilibrium position, i.e., $u_{\mathbf{i},\mu} = 0$. Ground state properties of this model will be studied using the Lanczos method³ on square clusters with periodic boundary conditions (PBC). The results will be presented on 4×4 clusters. Despite the small size we want to remark that

all previous exact numerical studies were carried out on smaller clusters, $\sqrt{8} \times \sqrt{8}$ in Ref.14 and $\sqrt{10} \times \sqrt{10}$ in Ref.13. In addition, larger tilted clusters do not possess the symmetry to fit horizontal or vertical stripes. Notice that the ionic displacements $u_{\mathbf{i},\mu}$ will be obtained by finding the configuration that minimizes the total energy²⁰ and without imposing *a priori* a given pattern for them. Details of the procedure were presented in Ref.20 and will not be repeated here.

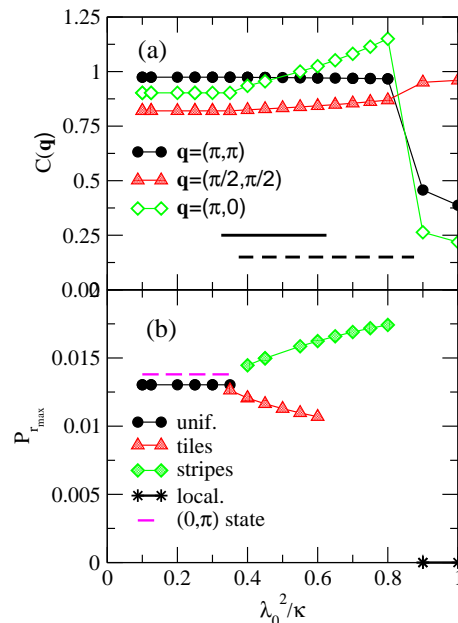


FIG. 1: Results for the diagonal breathing mode for four holes in a 4×4 lattice and $J = 0.4$. a) Charge structure factor for different values of the momentum \mathbf{q} as a function of the diagonal electron-phonon coupling. The full (dashed) line indicates the region where the tile (stripe) ground state is stable; b) Pairing correlations. The different symbols represent different ground states described in the text.

We will start by discussing the effects of the diagonal coupling, i.e., $\lambda_t = \lambda_J = 0$ in Eqs. (3) and (4). For the case of four holes, i.e., $\langle n \rangle = 0.75$ in a 4×4 lattice, we have observed that the ground state presents a uniform charge distribution up to $\lambda_0^2/\kappa = 0.3$. The probability of hole occupation $\langle n_h(\mathbf{i}) \rangle$ is the same for every site \mathbf{i} and the charge structure factor $C(\mathbf{q})$, shown in Fig. 1(a), does not have a sharp peak for any value of the momentum \mathbf{q} . Notice that the uniform ground state in the 4×4 lattice is three-fold degenerate, i.e. states with momentum $\mathbf{q} = (0, 0)$, $(\pi, 0)$ and $(0, \pi)$ have the same energy. The pairing²¹ correlations are not the same in these three degenerate uniform states. In Fig. 1(b) the filled

black circles indicate the averaged pairing correlations at the maximum distance along the diagonal. The pairing along the maximum diagonal distance for the state with momentum $(0, \pi)$ is indicated by the dashed line. For $\lambda_0^2/\kappa \geq 0.3$ the uniform ground state is replaced by a charge inhomogeneous state with a tiled structure schematically displayed in Fig. 2(a). The size of the circles is proportional to the probability of finding a hole in the corresponding site. The large circles indicate a probability of around 0.3 while the smaller ones correspond to about 0.2, which indicates that it is more likely to find the four holes in the tiles defined by the big circles than outside them. The state is stabilized by “extended breathing” modes as denoted by the arrows displayed in Fig. 2(a), which are proportional to the ionic displacements $u_{i,\mu}$. Although we are not aware of breathing or extended breathing modes being mentioned as relevant in the cuprates it is worth mentioning that so called “tiled” structures have been observed in STM experiments on $\text{Na}_x\text{Ca}_{2-x}\text{CuO}_2\text{Cl}_2$.²² In addition, all efforts to stabilize the observed tiled state in the t-J model without phonons have been unfruitful.²³ The pairing correlations in this state, denoted by the triangles in Fig. 1(b), are slightly suppressed but not destroyed. This state remains stable up to $\lambda_0^2/\kappa = 0.62$ but from $\lambda_0^2/\kappa \geq 0.38$ it coexists with a stripe state schematically shown in Fig. 2(b). As in the previous case, the large (small) circles indicate a site hole density of 0.3 (0.2) in the figure.

In agreement with neutron scattering results for the cuprates, four holes in the 4×4 lattice produce two stripes as opposed to only one.⁷ Also, in agreement with experimental data⁵, we observed that vertical (horizontal) stripes are stabilized by half-breathing modes along x (y). The ionic displacements for vertical stripes are presented in Fig. 2(b). The stripe state has a maximum in the charge structure factor at momentum $\mathbf{q} = (\pi, 0)$ (vertical stripes) or $(0, \pi)$ (horizontal stripes) which can be observed in Fig. 1(a). An interesting characteristic of the stripe state is that the pairing correlations at the maximum diagonal distance (filled diamonds in Fig. 1(b)) slightly increase when compared with the result obtained from the average of the three uniform states (filled circles). This result is important because it indicates that D-wave pairing correlations can survive in stripe-like states as long as the holes are mobile.

When the stripe-state is stabilized the triple degeneracy in momentum of the ground state is broken. The ground state is now a singlet with momentum $(0, \pi)$ ($(\pi, 0)$) for vertical (horizontal) stripes. The observed increase in the pairing correlations does not seem to arise due to the break down of the momentum degeneracy since the pairing correlations in the uniform state with momentum $(0, \pi)$ (dashed line in Fig. 1(b)) are weaker than in the stripe state. We have also observed that in the stripe state the pairing correlations are stronger in the direction perpendicular to the stripes than in the direction parallel to them.²⁴

The stripe state becomes the only ground state for

$0.6 \leq \lambda_0^2/\kappa \leq 0.8$. The magnetic structure factor $S(q)$ in the stripe state has a peak at $(\pi/2, \pi)$ which indicates a π -shift.

It is important to remark that a striped ground state has been very difficult to stabilize in the t-J model without using external fields or special boundary conditions.²⁵ However, our results show that a moderate diagonal electron-phonon coupling to breathing phononic modes stabilizes them in a wide region of parameter space. Local lattice distortions in the direction perpendicular to the stripe, i.e., half-breathing modes, are responsible for this. Coincidentally, these are the modes that most strongly couple to electrons in the cuprates.⁵

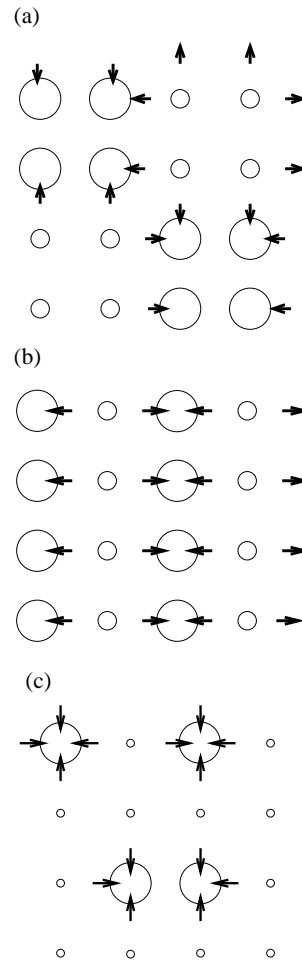


FIG. 2: (a) Schematic representation of the tile structure stabilized by extended breathing phononic modes; the radius of the circles is proportional to the hole density $x_i = 1 - n_i$ and the arrows represent the ionic displacements; (b) Schematic representation of the charge stripes stabilized by horizontal half-breathing phononic modes; (c) Schematic representation of the localized holes that result from large values of the diagonal electron-phonon coupling.

For $\lambda_0^2/\kappa > 0.8$ a state with localized holes, with one example schematically shown in Fig. 2(c), becomes the ground state. The holes are localized by displacements

of the neighboring ions as seen in the figure. The probability of finding a hole in the sites with the large (small) circles is almost 1 (0), which indicates that the holes are localized. The pairing correlations at long distance vanish in this state and they are indicated by the star symbols in Fig. 1(b).

For two holes ($\langle n \rangle = 0.875$) similar inhomogeneous charge structures were observed. As for the case of four holes, stripe states, shown in Fig. 3(a), are stabilized by half-breathing phononic modes. As before, the size of the circles is proportional to the probability of finding a hole in the corresponding site. Two holes induce one stripe in the 4×4 lattice in agreement with neutron scattering results.⁷ However, notice the different thickness of the arrows in Fig. 3(a) showing that the ionic displacements are stronger next to the holes. This state has a complicated structure in momentum space and the charge structure factors present peaks at $(\pi/2, 0)$, $(\pi, 0)$ and $(3\pi/2, 0)$. A tile structure with competing energy is also present in this case. The corresponding structure is shown in Fig. 3(b). Notice that although it is more likely to find the holes in the tile, the holes are not localized since there is a finite probability of finding them outside. The tendency towards pairing is clear because it is more likely that the two holes will be found along the stripe or inside the plaquette. Fully localized holes are observed for larger values of the diagonal electron-phonon coupling.

Qualitative changes are observed when 8 holes are introduced, i.e. at quarter filling. In agreement with earlier studies^{13,14} we found that the phonon mode that leads to the ground state in this case is the full-breathing mode that stabilizes a checkerboard charge density wave state, as shown in Fig. 4(a) for $J = 0.4$. The probability of finding holes associated to the size of the circles indicates that the holes are localized. The transition from the uniform state to the CDW state as a function of the diagonal coupling is characterized by a rapid increase of a peak at momentum (π, π) in the charge structure factor, shown in Fig. 5(a), and for the development of incommensurability, along the diagonal, in the magnetic structure factor (see Fig. 5(b)).

We have observed that for larger values of J , a dimer state, shown in Fig. 4(b) for $J = 1$, develops between the uniform and the CDW states. The new phase is clearly observed by monitoring the behavior of the charge structure factor, shown in Fig. 5(c) for $J = 1$. A peak at momentum $(\pi/2, \pi)$ develops because, as it can be seen in Fig. 4(b), the dimer state breaks rotational invariance. At the same time a peak at momentum $(\pi, 0)$ develops in the magnetic structure factor (see Fig. 5(d)). The dimer state is stabilized by extended breathing phonon modes for intermediate values of the EPI, i.e., $0.5 \leq \lambda_0^2/\kappa \leq 0.9$, for $J = 1$. The dimers are localized pairs. This state was not observed in previous studies which considered only local breathing modes.^{13,14} This result is not surprising since it is well known that the $t - J$ model presents phase separation at $J/t \geq 3$ in the absence of EPI. Thus, the proximity to phase separation causes the formation of

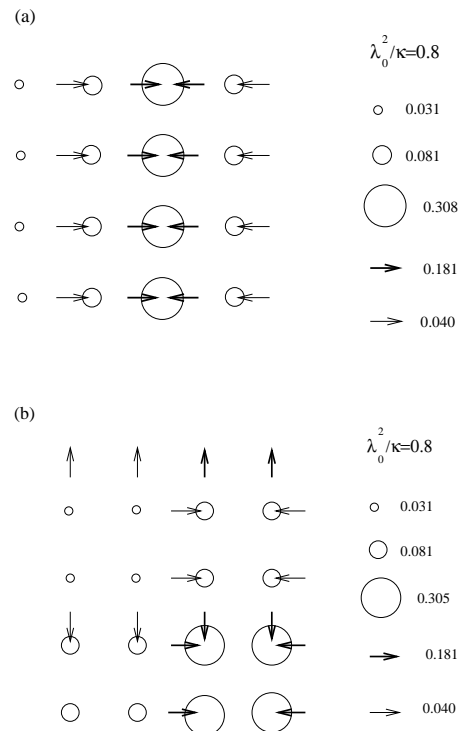


FIG. 3: (a) Schematic representation of the charge stripes stabilized by horizontal half-breathing phononic modes for 2 holes in a 4×4 lattice; the radius of the circles is proportional to the density of holes and the thickness of the arrows is proportional to the magnitude of the ionic displacements. (b) Same as (a) but for the tile structure stabilized by extended breathing phononic modes.

dimers at moderated values of λ_0^2/κ as J increases. For a fixed J the checkerboard CDW state is stabilized at sufficiently large values of the EPI.

The pairing correlations in the CDW and dimer states vanish at large distances which is not unexpected since in both cases the holes are localized.

In summary, the previous results show that the diagonal electron-phonon coupling to breathing modes stabilizes charge inhomogeneous structures, some of which, like stripes and tiles, have been observed in the cuprates. The pairing correlations are depressed when the holes are localized. However, in charge inhomogeneous states with *mobile* holes the D-wave pairing correlations survive. Although it is not possible to infer that long range correlations will develop in larger lattices, these results indicate that the interaction between magnetic and phononic degrees of freedom does not necessarily destroy pairing.

B. Buckling modes

For completeness, the effect of buckling modes will also be considered. Buckling modes are believed to be impor-

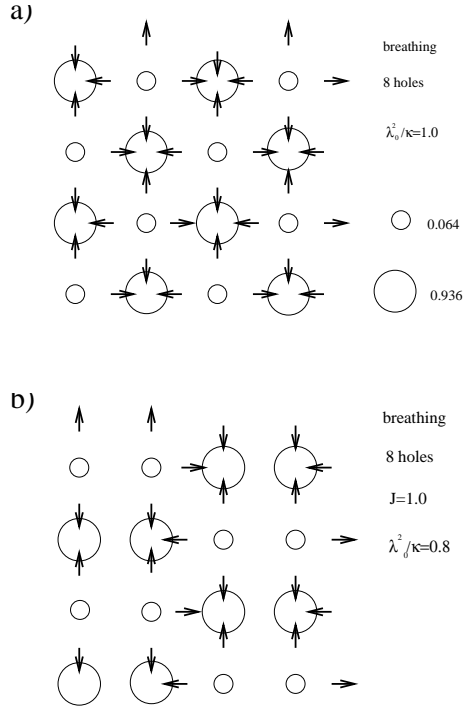


FIG. 4: (a) Schematic representation of the CDW state stabilized by breathing phononic modes using 8 holes in a 4×4 lattice for $J = 0.4$; (b) Schematic representation of the dimer state stabilized by extended breathing phononic modes at quarter filling (8 holes) for $J = 1$.

tant in YBCO^{12,26} and it was suggested that in combination with the magnetic interactions they could produce D-wave electronic pairing.¹¹ The buckling mode is incorporated by replacing $u(\mathbf{i})$ in Eq.(1) by

$$u(\mathbf{i}) = u_{i,x} + u_{i-\hat{x},x} + u_{i,y} + u_{i-\hat{y},y}, \quad (5)$$

while $t_{i,j}$ and $J_{i,j}$ have to be replaced by

$$t_{i,i+\mu} = t[1 + \lambda_t u_{i,\mu}], \quad (6)$$

and

$$J_{i,i+\mu} = J[1 + \lambda_J u_{i,\mu}]. \quad (7)$$

The most remarkable effects of adiabatic buckling modes are the following: 1) stripe and tile states qualitatively similar to the ones observed with half-breathing modes are stabilized in a very narrow region at intermediate values of the diagonal coupling, and 2) the ground state phase separates for large values of λ_0^2/κ .

We have observed the phase separated state by doping with 2, 4 and 8 holes. In the case of 2 holes pair localization appears. However, for 4 holes it can be seen that the holes localize in clusters instead of remaining isolated as it was the case with breathing modes (see

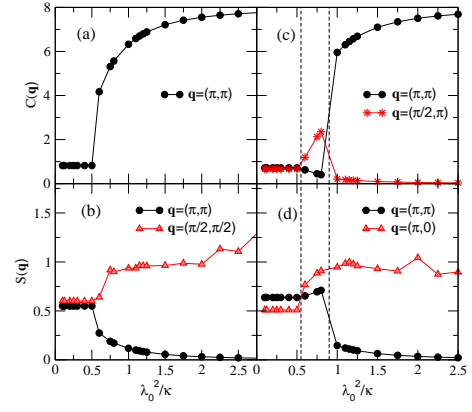


FIG. 5: (a) Charge structure factor for 8 holes in a 4×4 lattice for $J = 0.4$; (b) Magnetic structure factor for the same parameters as (a); (c) Same as (a) for $J = 1$; (d) same as (b) for $J = 1$.

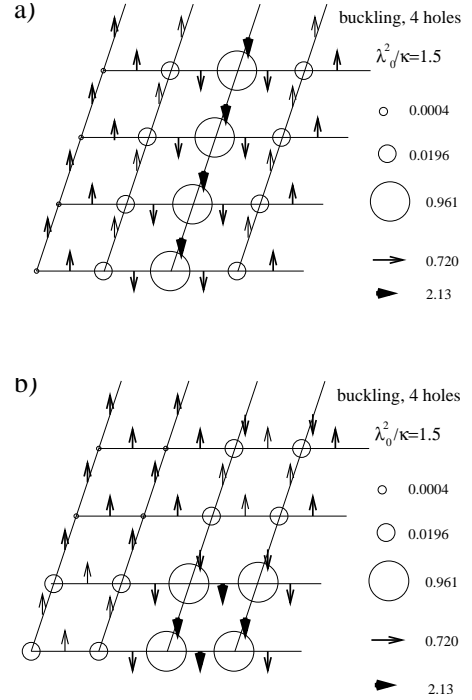


FIG. 6: Schematic representation of the phase separated states induced by buckling phononic modes for 4 holes in a 4×4 lattice: a) charge stripes; (b) the tile structure.

Fig. 2(c)). Examples of the phase separated clusters for 4 holes are shown in Fig. 6. The stripe (tile) structure in Fig. 6(a) (Fig. 6(b)) resembles the stripe (tiles) in Fig. 3(a) (Fig. 3(b)) obtained for 2 holes with breathing modes. However, we can see that the probability of hole occupation is almost 1 in the stripe and the tile inhomogeneities of Fig. 6 indicating localization. In the phase-separated state the holes are localized by strong

uniform displacements of the oxygens. In the case of the stripe, only the oxygens in the links along the stripe are strongly displaced while the tile is stabilized by a strong displacement of the oxygens in the links connecting the holes. In the interval $0.75 \leq \lambda_0^2/\kappa \leq 2.5$ the tile and the stripe states have very similar energies.

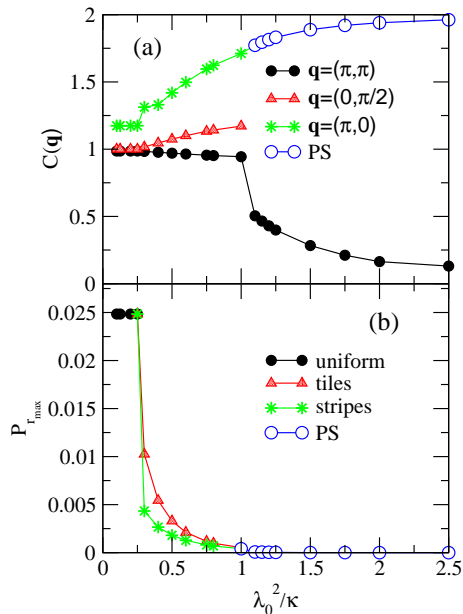


FIG. 7: (a) Charge structure factor as a function of the diagonal electron-phonon coupling for the buckling mode and 2 holes in a 4×4 lattice; (b) Pairing correlations at the maximum distance r_{max} for the same parameters as (a)

At quarter filling, i.e., 8 holes, it can be seen that the holes form a cluster so that two neighboring rows (or columns) in the 4×4 cluster have electrons and the other two rows (or columns) only have holes. Again, the holes are localized by strong displacements of the surrounding oxygens. As expected, the pairing correlations immediately vanish in the phase separated state.

Between the uniform and the phase separated states, a region with charge inhomogeneous structures is observed. For two holes we observe in Fig. 7(a) that a peak develops in the charge structure factor for $\lambda_0^2/\kappa = 0.25$. Tiles and stripes similar to those displayed in Fig. 3 become the ground state. As the coupling increases the holes become more and more localized in the stripe or the tile

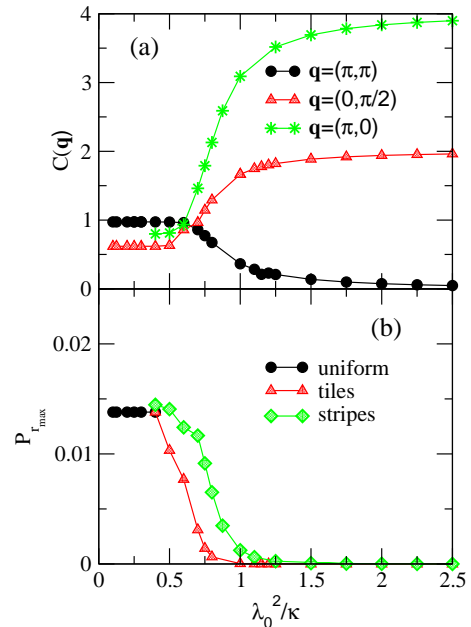


FIG. 8: (a) Charge structure factor as a function of the diagonal electron-phonon coupling for the buckling mode and 4 holes in a 4×4 lattice; (b) Pairing correlations at the maximum distance r_{max} for the same parameters as (a).

but phase separation occurs suddenly for $\lambda_0^2/\kappa \geq 1$ when the holes form a localized pair. In Fig. 7(b) it can be seen how the pairing correlations are reduced in the charge inhomogeneous phases as localization increases.

A similar behavior, displayed in Fig. 8, is observed for 4 holes. The remarkable result is that buckling modes appear to be able to stabilize the same kind of stripes than the half-breathing modes produce, but only in a very narrow region. Let us study in detail what is the underlying ionic configuration. In Fig. 9(a) we observe a schematic representation of the stripe state for $\lambda_0^2/\kappa = 0.4$. The hole density distribution is similar to the one for half-breathing modes shown in Fig. 2(b) but the ionic displacements are **not** the same. Clearly there is a break down of the rotational invariance so we could call the mode “half-buckling”. We notice that only the ions in the direction parallel to the stripes are displaced, while the breathing modes stabilize the stripe via displacements of the ions in the links perpendicular to the stripe. The oxygens in the links that connect the hole-rich sites move in one direction while those in the links that connect the hole poor sites move in the opposite direction.

This phononic configuration appears as an alternative to the half-breathing modes for stabilizing dynamic stripes but it is very unstable. The induced charge inhomogeneity is very small, of the order of 1%, and as we will see below, the state is rapidly replaced by a precursor of the phase-separated state.

For $\lambda_0^2/\kappa = 0.4$ a tile state is also stabilized. It is

shown in Fig. 9(b). We observe that only the oxygens in the links that connect the sites that form each tile are displaced. The oxygen displacements are opposite in hole rich and hole poor regions. It seems as if a depression in the position of the oxygen ions tends to localize the holes, like a depression in a mattress would tend to localize marbles. It is interesting to monitor how the stripe and tile configurations evolve to the phase separated states shown in Fig. 6. At $\lambda_0^2/\kappa = 0.5$ the stripes become distorted. An upward displacement of the oxygen ions along the last column in Fig. 10(a) effectively reduces the hole density in that column. A similar effect is observed in the tile state where, as we can see in Fig. 10(b), an upward displacement of the oxygens in one of the tiles pushes the holes out. We have observed that for $0.4 \leq \lambda_0^2/\kappa \leq 0.5$ the tile state has energy slightly lower than the stripe state.

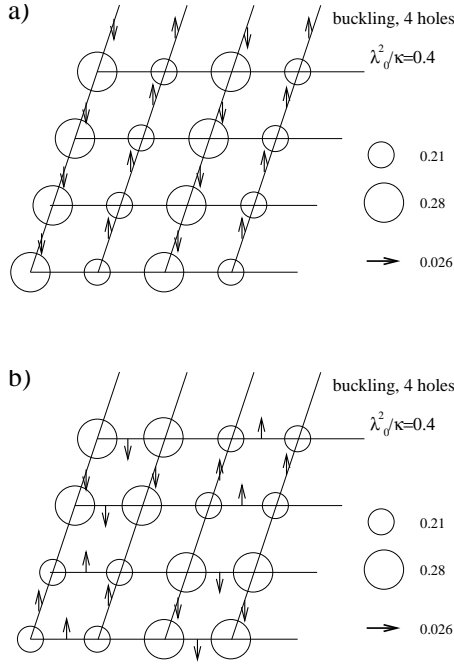


FIG. 9: (a) Schematic representation of the distorted charge stripes with weakly localized holes stabilized by buckling phononic modes for 4 holes in a 4×4 lattice at $\lambda_0^2/\kappa = 0.4$; (b) Same as (a) but for the tile structure.

An important qualitative change occurs at $\lambda_0^2/\kappa = 0.6$. Both in the stripe (Fig. 11(a)) and in the tile (Fig. 11(b))

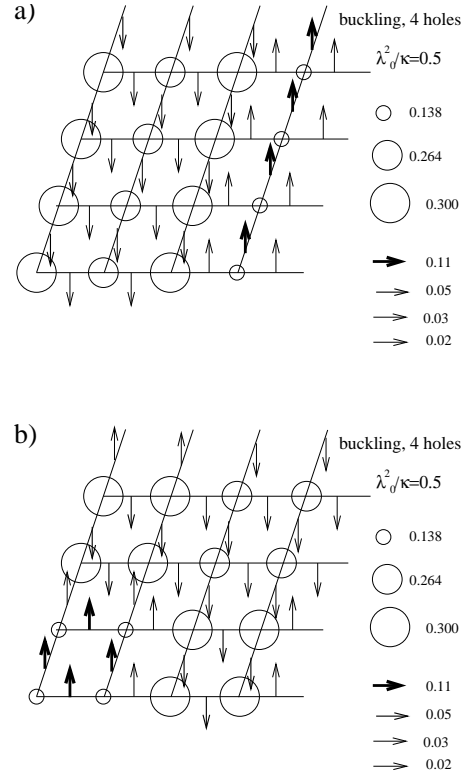


FIG. 10: (a) Schematic representation of the charge stripes stabilized by buckling phononic modes for 4 holes in a 4×4 lattice; (b) Same as (a) but for the tile structure stabilized by buckling phononic modes.

configurations the holes get localized in the region of the lattice in which the oxygens are depressed. The stripe state has the lowest energy in this case.

Finally, at $\lambda_0^2/\kappa = 0.7$ a structure similar to the one shown in Fig. 6 develops. The ion displacements become stronger as the diagonal coupling increases as well as the local differences in hole density. Actual phase separation, with $n(i) \approx 0$ or 1 in every site, i.e., with the holes completely localized, appears to develop for $\lambda_0^2/\kappa \geq 1$.

In Fig. 8(b) we can see the behavior of the pairing correlations in the different phases. It is interesting to compare with the corresponding results in Fig. 1(b) for the half-breathing case. The pairing correlations in the uniform state are, of course, the same as in Fig. 1(b). Thus, to simplify the figures we only present results for the state with momentum $(0, \pi)$ in the uniform case despite the fact that we know that the ground state is triply degenerate in momentum. The filled circles indicate the pairing along the maximum diagonal distance.

When the double stripe is stabilized for $\lambda_0^2/\kappa = 0.4$

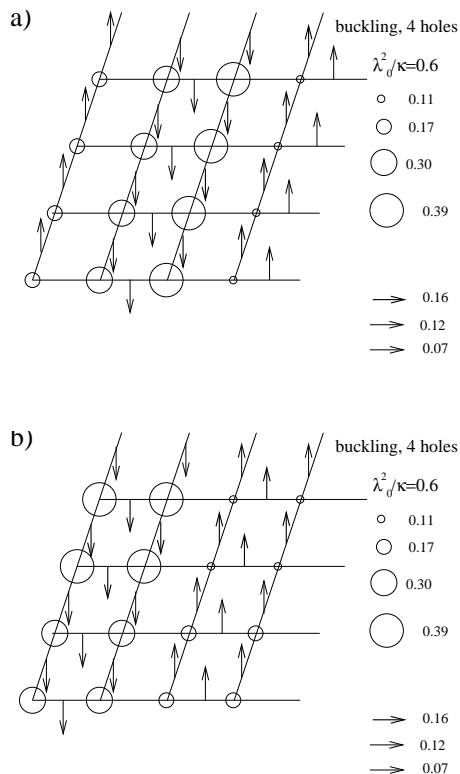


FIG. 11: (a) Schematic representation of the charge stripes, precursor of the phase separated state, stabilized by buckling phononic modes for 4 holes in a 4×4 lattice for $\lambda_0^2/\kappa = 0.6$; (b) Same as (a) but for the tile structure.

we observe a behavior very similar to the one for stripes in the breathing case. However, the stripes are destabilized by a phase which is a precursor of the phase separated state where the holes are localized by the buckling modes (see Fig. 10). The area of the localization region decreases with the diagonal EPI until the holes form a localized cluster and phase separation is reached. The pairing correlations, as expected, decrease sharply.

An interesting detail is that, as in the half-breathing case, in all stripe states the pairing correlation is larger in the direction perpendicular to the stripes than in the direction parallel to them.

At quarter filling the transition from the uniform to the phase-separated state is more abrupt. In fact, only for $\lambda_0^2/\kappa = 0.9$ the localization region is larger than two rows or columns. In Fig. 12(a) it is shown how the weak peak at (π, π) in the charge structure factor characteristic of the uniform ground state is replaced by a strong peak at $(0, \pi/2)$ indicating that half the lattice is filled with holes and the other half is empty. On the other hand, the magnetic incommensurability characteristic of the uniform quarter-filled state disappears in the phase separated region as it can be seen in Fig. 12(b).

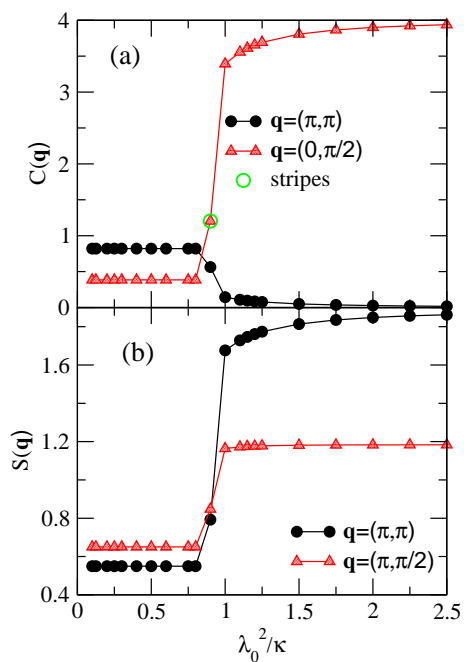


FIG. 12: (a) Charge structure factor as a function of the diagonal electron-phonon coupling for the buckling mode and 8 holes in a 4×4 lattice; (b) Magnetic structure factor for the same parameters as (a).

Summarizing, the buckling modes induce a lattice depression where the holes concentrate. A “half-buckling” mode that plays a role similar to the “half-breathing” mode is rapidly destabilized by the diagonal coupling in favor of a state with localized clustered holes and suppressed pairing correlations, which is a precursor of the phase-separated state.

C. Off-Diagonal Electron-Phonon coupling

At the adiabatic level, we have observed that the effect of the off-diagonal terms is to destabilize the charge inhomogeneous states with mobile holes that appear in between the uniform and the localized holes or phase separated phases. This can be seen in Fig. 13 where a phase diagram in the plane λ_t vs λ_0^2/κ for breathing modes is presented for 4 holes and $\lambda_J = \lambda_t$. It can be seen that for $\lambda_0^2/\kappa \approx 0.7$ the charge inhomogeneous stripe/tile state is replaced by an uniform ground state for $\lambda_t = 0.1$. As λ_0 increases, larger values of λ_t are needed to restore the uniform ground state. The region labeled *M* in the figure is characterized by charge inhomogeneous states with mobile holes. This phase is overcome by the uniform state for larger values of the off-diagonal coupling. We have not observed any enhancement of the pairing correlations due to the off-diagonal coupling.

For buckling modes, see Fig. 14, we observe that small values of λ_t just renormalize the diagonal coupling to a

smaller value so that the uniform ground state remains stable up to larger values of λ_0^2/κ . However, larger values of λ_t destabilize the inhomogeneous phase with mobile holes labeled M in the figure, and for $\lambda_t > 0.2$ the system goes from a uniform to a phase separated state as a function of λ_0^2/κ .

The off-diagonal coupling does not generate new phases, it simply seems to renormalize the diagonal coupling. In fact, its effect is to destabilize the inhomogeneous phase with mobile holes identified by M in Figs. 13 and 14. This phase is more easily destabilized for buckling than for breathing modes.

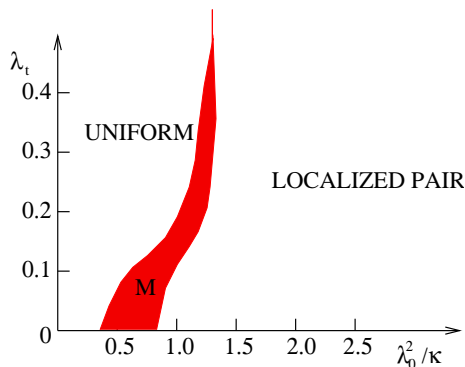


FIG. 13: Phase diagram for 4 holes as a function of the diagonal EPI λ_0^2/κ and the off-diagonal coupling λ_t for breathing modes. In this case $\lambda_J = \lambda_t$. M characterizes charge inhomogeneous states with mobile holes described in the text.

III. QUANTUM PHONONS

The results presented in the previous section indicate that the phonon mode that most closely reproduces the experimental results observed in the cuprates is the half-breathing. In addition, neutron scattering experiments show that this is the mode the most strongly coupled to the charge in the high T_c cuprates. For this reason we decided to study the effects of the half-breathing mode beyond the adiabatic approximation.

In order to study the electron-phonon interaction at finite frequency the electron-phonon part of the Hamil-

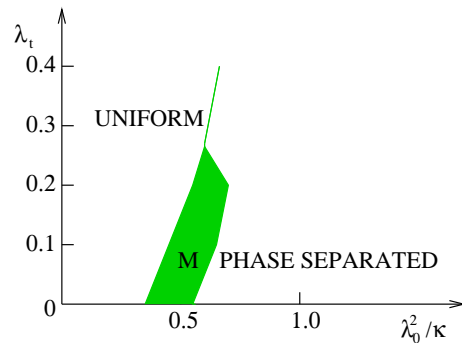


FIG. 14: Phase diagram for 4 holes as a function of the diagonal EPI λ_0^2/κ and the off-diagonal coupling λ_t for buckling modes. In this case $\lambda_J = \lambda_t$. M characterizes charge inhomogeneous states with mobile holes described in the text.

tonian (Eq.(1b)) should be replaced by¹⁴

$$H_{e-ph} = \lambda_0 \sum_{\mathbf{i}, \mu} (b_{\mathbf{i}, \mu}^\dagger + b_{\mathbf{i}, \mu}) (n_{\mathbf{i}} \mp n_{\mathbf{i}+\mu}), \quad (8a)$$

where the minus sign between the densities corresponds to the breathing mode while the plus sign corresponds to the buckling mode that will be discussed later. $b_{\mathbf{i}, \mu}^\dagger$ creates a phonon at the link \mathbf{i}, μ with frequency ω and $\lambda_0 = g\sqrt{\frac{1}{2m\omega}}$, where g is the electron-phonon coupling and m is the ionic mass. Eq.(1c) should be replaced by

$$H_{ph} = \omega \sum_{\mathbf{i}, \mu} (b_{\mathbf{i}, \mu}^\dagger b_{\mathbf{i}, \mu} + \frac{1}{2}). \quad (8b)$$

The off-diagonal effects are given by

$$t_{\mathbf{i}, \mathbf{j}} = t\{1 + \lambda_t[\hat{B}(\mathbf{i}) + \hat{B}(\mathbf{j})]\}, \quad (9)$$

and

$$J_{\mathbf{i}, \mathbf{j}} = J[1 + \lambda_J[\hat{B}(\mathbf{i}) + \hat{B}(\mathbf{j})]\}, \quad (10)$$

where

$$\hat{B}(i) = b_{\mathbf{i}, \mathbf{x}} + b_{\mathbf{i}, \mathbf{x}}^\dagger - b_{\mathbf{i}-\hat{\mathbf{x}}, \mathbf{x}} - b_{\mathbf{i}-\hat{\mathbf{x}}, \mathbf{x}}^\dagger + b_{\mathbf{i}, \mathbf{y}} + b_{\mathbf{i}, \mathbf{y}}^\dagger - b_{\mathbf{i}-\hat{\mathbf{y}}, \mathbf{y}} - b_{\mathbf{i}-\hat{\mathbf{y}}, \mathbf{y}}^\dagger. \quad (11)$$

In order to simplify these expressions we make the Fourier transform of phonon and electron operators. Then, in momentum space, the interaction term becomes:

$$H_{e-ph} = \frac{1}{\sqrt{N}} \sum_{\mathbf{k}, \mathbf{q}, \mu, \sigma} \lambda_0 (1 \mp e^{-i\mathbf{q}\cdot\hat{\mu}}) c_{\mathbf{k}, \sigma}^\dagger c_{\mathbf{k}-\mathbf{q}, \sigma} (b_{\mathbf{q}, \mu}^\dagger + b_{-\mathbf{q}, \mu}). \quad (12)$$

The effective electron-phonon coupling constant $\lambda(\mathbf{q}, \mu) = \lambda_0 (1 \mp e^{-i\mathbf{q}\cdot\hat{\mu}})$ is clearly anisotropic. For breathing modes (negative sign inside the parenthesis) it is strongest for $\mathbf{q}_{max} = (\pi, \pi)$ and, thus, in the simplest approximation only the phonon mode $b_{\mathbf{q}_{max}}$ is

maintained.^{13,14} For half-breathing modes $\mathbf{q}_{max} = (\pi, 0)$ or $(0, \pi)$. Under this approximation the Hamiltonian for half-breathing modes along x becomes:

$$H_{e-ph}^{br} = 2\lambda_0(b^\dagger + b) \sum_{\mathbf{i}} n_{\mathbf{i}}(-1)^{x_{\mathbf{i}}}, \quad (13)$$

where $x_{\mathbf{i}}$ is the x -coordinate of site \mathbf{i} .

$$H_{ph}^{br} = \omega(b^\dagger b + \frac{1}{2}). \quad (14)$$

The off-diagonal effects on the hopping and the Heisenberg coupling vanish along the direction of the half-breathing modes (\hat{x} in this case). Along the perpendicular direction they are given by

$$t_{\mathbf{i},\mathbf{i}+\hat{y}}^{br} = t[1 + 4\lambda_t(-1)^{x_{\mathbf{i}}}(b^\dagger + b)], \quad (15)$$

and

$$J_{\mathbf{i},\mathbf{i}+\hat{y}}^{br} = J[1 + 4\lambda_J(-1)^{x_{\mathbf{i}}}(b^\dagger + b)]. \quad (16)$$

This behavior was also remarked in Ref.16.

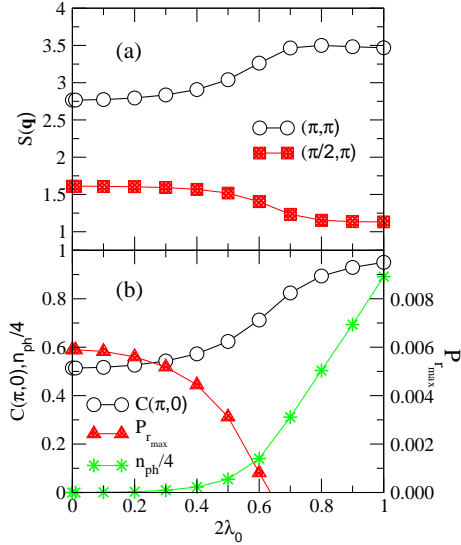


FIG. 15: (a) Magnetic structure factor for different values of the momentum as a function of the diagonal electron-phonon coupling, for quantum half-breathing modes in a 4×4 lattice for 2 holes. (b) Charge structure factor, pairing at maximum distance, and average number of phonons as a function of the diagonal electron-phonon coupling, for quantum half-breathing modes in a 4×4 lattice with 2 holes.

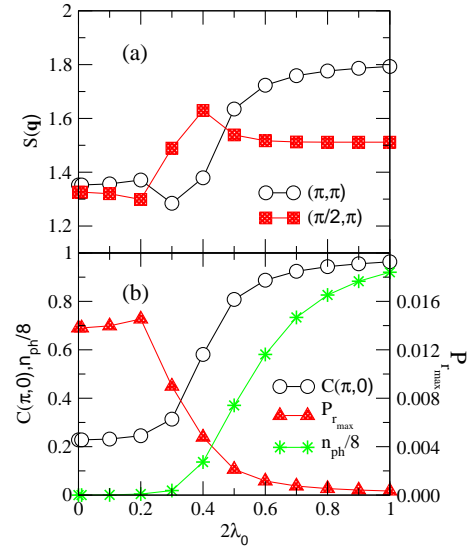


FIG. 16: (a) Magnetic structure factor for different values of the momentum as a function of the diagonal electron-phonon coupling, for quantum half-breathing modes in a 4×4 lattice for 4 holes. (b) Charge structure factor, pairing at maximum distance and average number of phonons as a function of the diagonal electron-phonon coupling, for quantum half-breathing modes in a 4×4 lattice for 4 holes.

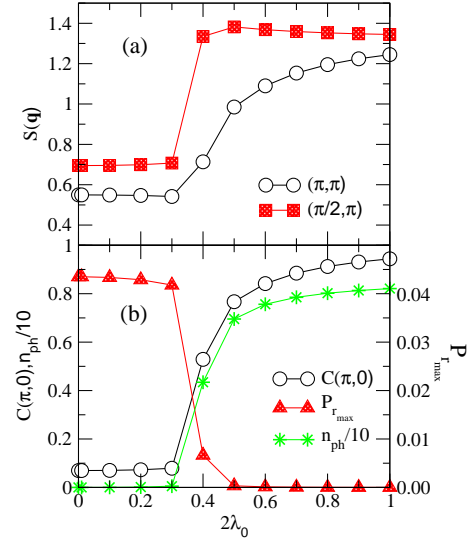


FIG. 17: (a) Magnetic structure factor for different values of the momentum as a function of the diagonal electron-phonon coupling for quantum half-breathing modes in a 4×4 lattice for 8 holes. (b) Charge structure factor, pairing at maximum distance and average number of phonons as a function of the diagonal electron-phonon coupling for quantum half-breathing modes in a 4×4 lattice for 8 holes.

As in the previous sections, J will be fixed to 0.4; ω will be set to 1.

Let us discuss first the effects of the diagonal coupling, i.e., $\lambda_t = \lambda_J = 0$. An important difference between the adiabatic and the quantum case is that with adiabatic phonons the ionic displacements were unconstrained and, as a result, we observed that in some regions of parameter space extended breathing modes with rotational symmetry that stabilized tile, CDW, and localized holes structures, were energetically more favorable than half-breathing modes. With quantum phonons, we will study half-breathing modes only and, thus, all the charge inhomogeneous states that will arise will be stripe-like.

In Fig. 15 results for 2 holes doped in a 4×4 lattice are presented. In panel (a) we observe the magnetic structure factor for different values of the momentum. It can be seen that the value at (π, π) is always maximum and, as a result, magnetic incommensurability does not develop. The charge structure factor (open circles in panel (b)) indicates that a stripe-like structure starts to develop at $2\lambda_0 = 0.5$, i.e., when the average number of phonons (star symbols) becomes different from zero. However, the pairing correlations at the maximum diagonal distance (indicated by triangles) always decrease for finite EPI and actually vanish in the stripe phase. This occurs because the stripe pattern that results in this case is different from the physically “correct” stripe shown in Fig. 3(b) that we obtained in the adiabatic case. In order to obtain this pattern with quantum phonons, finite values of $g(\pi/2, 0)$ should be considered in addition to finite values of $g(\pi, 0)$, as explained in Section II. The single coupling at momentum $(\pi, 0)$ stabilizes a double stripe pattern with one hole per stripe. The charge difference between the background and stripes is large enough to develop a peak at $(\pi, 0)$, but the behavior of the magnetic structure factor indicates that it does not produce a π -shift.

In Fig. 16, results for different values of λ_0 on a 4×4 lattice doped with four holes are presented. In this case we obtain results qualitatively very similar to those in the adiabatic case (Fig. 1). The magnetic structure factor displayed in Fig. 16(a) develops a peak at $\mathbf{q} = (\pi/2, \pi)$ for $0.2 < 2\lambda_0 < 0.5$, which indicates that a state with magnetic incommensurability is stabilized. The charge structure factor shown in Fig. 16(b) (with open circles) indicates that charge order consistent with two vertical stripes develops in the magnetically incommensurate region. The uniform ground state is replaced by an inhomogeneous one when the number of phonons (star symbols) becomes finite at $2\lambda_0 > 0.2$. This is similar to the effect observed with adiabatic phonons. For $2\lambda_0 > 0.5$ the charge structure factor results indicates that a static stripe-like structure has developed. A π -shift does not occur since $S(\mathbf{q})$ has a maximum at (π, π) .

A small enhancement in the pairing correlations at maximum diagonal distance (triangles in Fig. 16(b)) occurs as a function of λ_0 in the uniform phase. As in the adiabatic case, D-wave pairing correlations are **not** dra-

matically affected in charge inhomogeneous states with mobile holes.

Fig. 17 shows the results at quarter-filling. Instead of a CDW stabilized by full-breathing modes, which is what we observed in the adiabatic case, the half-breathing modes still generate a two-stripe structure. This occurs because we are still studying the effects of half-breathing modes, while phonon operators with momentum (π, π) would induce the CDW state. The strong peak in the charge structure factor C at $(\pi, 0)$ (open circles in Fig. 17(b)) underlines the large charge inhomogeneity which induces magnetic incommensurability, as it can be seen from the magnetic structure factor’s behavior displayed in Fig. 17(a).

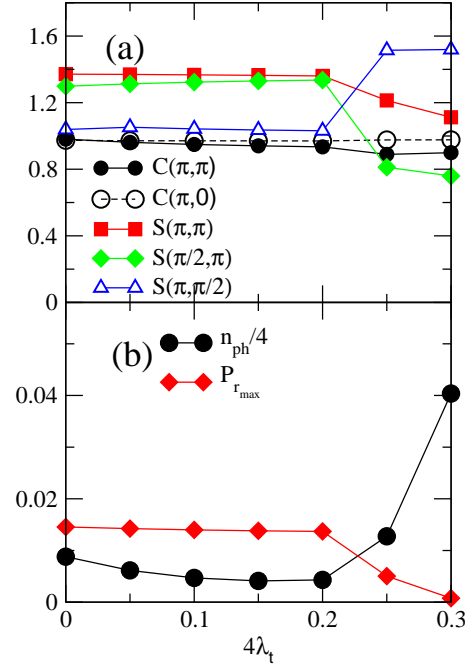


FIG. 18: (a) Charge (C) and Magnetic (S) structure factors for different values of the momentum, as a function of the off-diagonal electron-phonon coupling λ_t for quantum half-breathing modes in a 4×4 lattice for 4 holes. $\lambda_J = 2\lambda_t$ and the diagonal coupling is given by $2\lambda_0 = 0.2$. (b) Pairing at maximum diagonal distance, and average number of phonons as a function of the off-diagonal electron-phonon coupling for quantum half-breathing modes for the same parameters as in part (a).

The tendency to incommensurate order increases as the doping is increased from 2 to 8 holes, as it can be seen in Figs. 15, 16 y 17 ((a) panels). This is understandable since the antiferromagnetic ordering between

the two undoped domains outside the stripes is reduced when the stripes become increasingly populated by holes.

Let us now consider the effects of off-diagonal electron-phonon coupling. We will start with the case of 4 holes at $2\lambda_0 = 0.2$ which, according to Fig. 16(b), provides the state with the strongest pairing correlations. We have set $\lambda_J = 2\lambda_t$.¹⁶ The state at $\lambda_t = 0$ is uniform and, like in the adiabatic case (Fig. 1), is triply degenerate in momentum. The off-diagonal EPI breaks the degeneracy in momentum and selects the ground state with momentum $(0, \pi)$. As λ_t increases the peak in the charge structure factor at momentum $(\pi, 0)$ remains almost unchanged (circles in Fig. 18(a)). The peaks at momentum (π, π) (squares) and $(\pi/2, \pi)$ (diamonds) in the magnetic structure factor remains essentially unchanged as well. While this happens the pairing correlations and the average number of phonons decrease slightly (Fig. 18(b)). This trend continues up to $4\lambda_t = 0.2$. Beyond this value, there are no indications of the formation of a charge inhomogeneity but there are some changes in the magnetic channel with an incipient order with momentum $(\pi, \pi/2)$.

We will also study the effects of off-diagonal interactions for $2\lambda_0 = 0.4$, i.e., in the region with dynamical stripes. The effect of λ_t in this case is to select the state with momentum $(0,0)$ as the ground state. At $\lambda_t = 0$ the ground state presents a charge inhomogeneous state with two stripes according to the large peak at $(\pi, 0)$ in $C(\mathbf{q})$ (circles in Fig. 19(a)) exhibiting magnetic incommensurability. The pairing is very reduced. As λ_t increases up to $4\lambda_t = 0.1$ the charge inhomogeneity is reduced and the pairing correlations increase indicating that λ_t is renormalizing λ_0 making it effectively smaller and stabilizing the charge uniform state. This is clearly seen at $4\lambda_t = 0.15$ when the ground state changes momentum to $(\pi, 0)$ and we observed a ground state with properties similar, including the pairing, to the case $\lambda_0 = 0.2$ and $\lambda_t = 0$. The off-diagonal coupling just seems to make the diagonal one weaker.

This level crossing is related to the disappearance of the magnetic incommensurability at $(\pi/2, \pi)$. Once this incommensurability has disappeared, a second level crossing takes place at $4\lambda_t \approx 0.225$ and the ground state momentum is again $(0,0)$. By further increasing λ_t , the charge ordering is reestablished. This complex behavior, together with the one previously found for $2\lambda_0 = 0.2$, illustrates the interplay between the diagonal and off-diagonal EPI. In particular, due to a nonzero λ_J , the spin degrees of freedom are now directly coupled to the ion displacements, and hence magnetic orderings are more relevant to the overall behavior than with purely diagonal EPI.

For completeness we are going to comment on the effects of the diagonal electron-phonon coupling to buck-

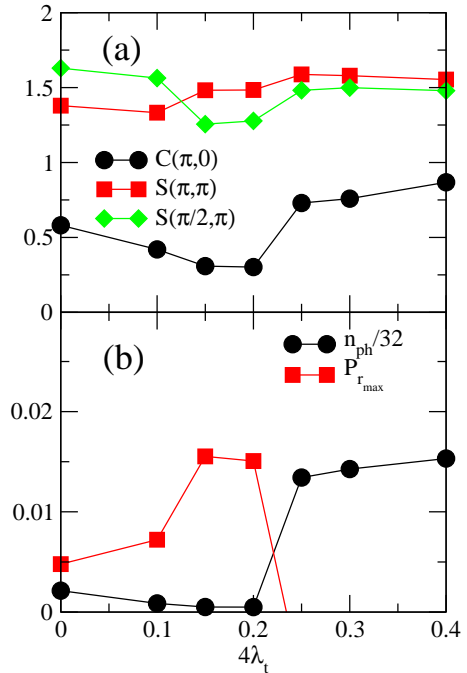


FIG. 19: (a) Charge and magnetic structure factor for different values of the momentum as a function of the off-diagonal electron-phonon coupling λ_t for quantum half-breathing modes in a 4×4 lattice for 4 holes. $\lambda_J = 2\lambda_t$ and the diagonal coupling is given by $2\lambda_0 = 0.4$. (b) Pairing at maximum diagonal distance, and average number of phonons as a function of the off-diagonal electron-phonon coupling for quantum half-breathing modes for the same parameters as in part (a).

ling modes with quantum phonons.

Our studies with adiabatic phonons showed that in a very narrow region of parameter space stripes were stabilized by a buckling mode that breaks rotational invariance. The mode that stabilizes vertical stripes would have a maximum coupling constant at momentum $(\pi, 0)$. Selecting this momentum in Eq.(12) (with the plus sign) we arrive to the same Hamiltonian as in the half-breathing case, except that the single phonon modes are now along the y direction (parallel to the stripe) rather than in the direction x as in the half-breathing case, in agreement with the results obtained in the adiabatic case (Fig. 9(a)). In addition, off-diagonal effects vanish in this case. Thus, the same physical properties as in the diagonal half-breathing case are obtained.

In Ref. 11 it was shown at the mean-field level that a diagonal coupling was sufficient to enhance D-wave pairing correlations. Selecting the plus sign in Eq.(12) we observe that the effective coupling constant is maximum for $\mathbf{q} = (0, 0)$ and vanishes at momentum (π, π) in agreement with the result of Nazarenko et al.¹¹. Regretfully

keeping only momentum $\mathbf{q} = (0, 0)$ in Eq.(12) leads to

$$H_{e-ph}^b = 2\lambda_0 \sum_{\mu} (b_{\mu}^{\dagger} + b_{\mu}) \sum_{\mathbf{i}} n_{\mathbf{i}}, \quad (17)$$

and

$$H_{ph}^b = \omega \sum_{\mu} (b_{\mu}^{\dagger} b_{\mu} + \frac{1}{2}), \quad (18)$$

which does not couple the electrons to the phonons since the number of electrons is fixed in our simulations and $\sum_{\mathbf{i}} n_{\mathbf{i}}$ is constant for all states. A study of this case conserving more than two phonon modes would be desirable since mean field calculations¹¹ and results for 2 holes doping obtained with a truncated approach¹⁴ provided encouraging results towards D-wave pairing stabilization.

IV. CONCLUSIONS

Summarizing, we have studied the effects of electron-phonon interactions in the t-J model for a variety of phononic modes, couplings, and electronic densities using small clusters solved exactly. The most remarkable result is that charge inhomogeneous states with mobile holes are stabilized by these interactions. In particular, stripe states which are very difficult to stabilize in the t-J model are clearly observed. Tile structures, detected experimentally in some cuprates, are stabilized for the

first time in the t-J model. Our calculations also confirm that the half-breathing mode that stabilizes the stripes is the most energetically favorable in some regions of parameter space. We have also found that buckling modes can generate stripe and tile states in a very narrow range of electron-phonon coupling constants. Thus, this mode also has to be considered in the interpretation of experimental data. The pairing correlations vanish in the regime of localized holes induced by the EPI but it is encouraging that not drastic effects occur in the states with mobile holes. In fact, small enhancements have been detected in some cases. This should be contrasted with the pair breaking effects of the full breathing mode in D-wave superconductors. As previously observed in the context of the spin-fermion model²⁴ and diagrammatic calculations,²⁷ diagonal EPI induce charge localization while off-diagonal EPI encourages hole mobility.

Our results indicate that electron-phonon interactions need to be considered in order to understand the properties of the high-Tc cuprates, in particular, the existence of charge inhomogeneous ground states.

V. ACKNOWLEDGMENTS

We acknowledge discussions with T. Egami, J. Tranquada, G. Sawatzky and E. Dagotto. A.M. is supported by NSF under grants DMR-0443144 and DMR-0454504. Additional support is provided by ORNL.

-
- ¹ J.Bardeen, L.N. Cooper and J.R. Schrieffer, Phys. Rev. **108**, 1175 (1957).
² P.W. Anderson and J.R. Schrieffer, Phys. Today **44** 55 (1991).
³ E. Dagotto, Rev. Mod. Phys.**66**, 763 (1994) and references therein.
⁴ A. Bianconi, N.L. Saini, A. Lanzara, M. Missori, T. Rossetti, H. Oyanagi, H. Yamaguchi, K.Oka and T. Ito, Phys. Rev. Lett. **76** 3412 (1996).
⁵ R.J. McQueeney, Y. Petrov, T. Egami, M.Yethiraj, G, Shirane and Y. Endoh, Phys.Rev.Lett.**82**, 628 (1999).
⁶ A. Lanzara, P. V. Bogdanov, X. J. Zhou, S. A. Kellar, D. L. Feng, E. D. Lu, S. Uchida, H. Eisaki, A. Fujimori, K. Kishio, J.-I. Shimoyama, T. Noda, S. Uchida, Z. Hussain, and Z.-X. Shen, Nature **412**, 510 (2001).
⁷ J.M. Tranquada, D.J. Buttrey, V. Sachan and J.E. Lorenzo, Phys.Rev.Lett.**73**, 1003 (1994); J.M. Tranquada, R. Mallozi, J. Orenstein, T.N. Eckstein and I. Bozovic, Nature (London) **375**, 561 (1995).
⁸ K. McElroy, R.W. Simmonds, J.E. Hoffman, D.-H. Lee, J. Orenstein, H. Eisaki, S. Uchida, and J.C. Davis, Nature **422**, 520 (2003).
⁹ M. Vershinin, S. Misra, S. Ono, Y. Abe, Y. Ando, and A. Yazdani, www.scienceexpress.org, 10.1126/science.1093384.
¹⁰ E. Dagotto, T. Hotta and A. Moreo, Phys. Rep. **344**, 1 (2001). See also A. Moreo, S. Yunoki and E. Dagotto, Phys.Rev.Lett.**83**, 2773 (1999); T. Hotta, A. Malvezzi and E. Dagotto, Phys. Rev. B **62**, 9432 (2000).
¹¹ A. Nazarenko and E. Dagotto, Phys. Rev. B **53**, R2987 (1996).
¹² J. Song and J.F. Annett, Phys. Rev. B **51**, 3840 (1995); **52**, 6930(E) (1995).
¹³ A. Dobry, A. Greco, S. Koval and J. Riera, Phys. Rev. B **52**, 13722 (1995).
¹⁴ T. Sakai, D. Poilblanc and D.J. Scalapino, Phys. Rev. B **55**, 8445 (1997).
¹⁵ T. Egami and S. Billinge, Physical Properties of High Temperature Superconductors V, ed. D. M. Ginsberg (World Scientific, Singapore), page 265 (1996).
¹⁶ S. Ishihara and N. Nagaosa, Phys. Rev. B **69**, 144520 (2004).
¹⁷ O. Rösch and O. Gunnarsson, Phys. Rev. Lett. **92**, 146403 (2004).
¹⁸ T.P. Devereaux, T. Cuk, Z-X. Shen and N. Nagaosa, Phys. Rev. Lett. **93**, 11704 (2004).
¹⁹ K. Yonemitsu, A.R. Bishop and J. Lorenzana, Phys. Rev. B **47**, 8065 (1993).
²⁰ A. Dobry and J. Riera, Phys. Rev. **B 56**, R2912 (1997); A. E. Feiguin, J. A. Riera, A. Dobry, and H. A. Ceccatto Phys. Rev. **B 56**, 14607 (1997).
²¹ The pairing correlations presented in this paper are D-wave which are the most enhanced in the t-J model without phonons. We have also studied extended-S and P-wave pairings but these correlations are always weaker than the

- D-wave ones.
- ²² T. Hanaguri, C. Lupien, Y. Kohsaka, D.-H. Lee, M. Azuma, M. Takano, and J.C. Davis, *Nature (London)* **430**, 1001 (2004).
- ²³ S. R. White, private communication.
- ²⁴ A similar behavior was observed in a spin-fermion model. M. Moraghebi, S. Yunoki and A. Moreo. *Phys. Rev. Lett.* **88**, 187001 (2002); Y. Yildirim and A. Moreo, *Phys. Rev. B* **72**, 134516 (2005).
- ²⁵ S.R. White and D.J. Scalapino, *Phys. Rev. Lett.* **80**, 1272 (1998); S.R. White and D.J. Scalapino, *Phys. Rev. Lett.* **81**, 3227 (1998).
- ²⁶ B. Normand, H. Kohno, and H. Fukuyama, *Phys. Rev. B* **53**, 856 (1996).
- ²⁷ A.S. Mishchenko and N. Nagaosa, *Phys. Rev. Lett.* **93**, 036402 (2004).